

TEMPERATURE EFFECTS ON ROLLING TEXTURE FORMATION IN ZIRCONIUM ALLOYS

A.A. Pochettino¹, P. Sánchez¹, R. Lebensohn² and C.N. Tome³

¹ Dpto. Materiales, Gcia. Desarrollo, CNEA,
Av. Libertador 8250, 1429 Buenos Aires, Argentina

² IFIR, UNR-CONICET, Av. Pellegrini 250, 2000 Rosario, Argentina

³ Reactor Materials Research Branch, Whiteshell, Lab., AECL, Pinawa, ROE1LO, Manitoba,
Canada

Keywords: Texture, Zirconium, Rolling, Temperature, Slip, Twinning

ABSTRACT:

The effect of the different deformation modes on the development of the rolling texture in Zr alloys at different temperatures was analyzed by comparing theoretical predictions with experimental results of texture evolutions. Calculations were performed using the Viscoplastic Self-consistent (SC) Model, and twinning reorientation was treated by means of the Volume Fraction Transfer (VFT) scheme. In order to obtain an accurate representation of rolling textures, a systematic analysis of the active deformation modes, as well as their Critical Resolved Shear Stress (CRSS) dependence with temperature and their effects on the texture formation was carried out.

INTRODUCTION

During mechanical transformations in Zirconium alloys, the prismatic $\langle a \rangle$ or $\{1100\} \langle 1120 \rangle$ slip is the most active mode in a wide range of temperatures [1-2]. Nevertheless, since prismatic slip does not suffice for accommodating an arbitrary imposed strain, other deformation modes must be activated: $\{1012\} \langle 1011 \rangle$ 'tensile' twinning (tw) and $\{1011\} \langle 1123 \rangle$ 'compressive' twinning (ctw) are mostly active at low and intermediate temperatures whereas non-prismatic slip modes become active at high temperatures. In this case, Pyramidal $\langle c+a \rangle$ or $\{1011\} \langle 1123 \rangle$, pyramidal $\langle a \rangle$ or $\{1101\} \langle 1120 \rangle$ and basal $\langle a \rangle$ or $(0001) \langle 1120 \rangle$ slip can complement the deformation pattern [3].

The purpose of this paper is to analyze the effect of the different deformation modes on the development of the rolling texture in Zr alloys at different temperatures. The study is performed by the comparison of theoretical predictions with experimental results of texture evolutions. Calculations were performed using the Viscoplastic Selfconsistent (SC) Model. In order to obtain an accurate representation of rolling textures, a systematic analysis of the

active deformation modes as well as their Critical Resolved Shear Stress (CRSS) dependence with temperature and their effects on the texture formation was carried out. CRSS values were chosen accounting data from literature which assure the best agreement with experiments. Texture predictions results show the importance of taking into account grain interactions in order to give a more realistic description of polycrystal plasticity in a wide range of temperature.

CALCULATIONS OF TEXTURE DEVELOPMENT

The calculation of texture development must be based on a reliable hypothesis about the way in which the polycrystal strain rate and stress $\dot{\epsilon}$ and Σ , respectively- and the corresponding magnitudes of the constituent grains ϵ and σ - are correlated. The SC formulation with a viscoplastic constitutive equation ($n=19$ and $n=7$ for cold and hot deformation respectively) is used [4]. As it is well known, the SC formulation allows each grain to deform differently, according to its directional properties and depending on the strength of the interaction between the grain and its surroundings. Twinning reorientation is treated by means of the Volume Fraction Transfer (VFT) scheme [5]. This method allows to keep track of the exact twinned volume by keeping constant the number orientations along the calculations.

Results starting from a random texture (Bunge-Roe description - Euler angles Ψ, θ, ϕ) with a final true strain $\epsilon=1$ (63% thickness reduction) are reported here. The set of CRSS values for the different deformation modes were selected considering those simulations which present the better agreement with experimental pole figures of cold and hot-rolled Zr alloys. Figure 1 shows different experimental and predicted (0002) pole figures. A good agreement between them can be observed for the CRSS values:

Cold rolling	Hot rolling
$\tau_{pr<a>} = 1, \tau_{tw} = 1.25, \tau_{ctw} = 2.5$	$\tau_{pr<a>} = 1, \tau_{b<a>} = 1.5, \tau_{py<c+a>} = 4$

The choice of these CRSS values was discussed in previous papers [4] [6]. Some differences exist between experimental textures measured by different authors [7-8-9]. They can be associated to different alloy contents and deformation histories. In Fig. 1.(a) and (c), we present the most typical experimental low (LT) and high (HT) temperature textures.

RESULTS AND DISCUSSION

COLD ROLLING TEXTURES:

The predicted texture presents a good agreement with experimental results, as it can be observed in the (0002) pole figures, Fig. 1. Table 1 shows the relative activity of the different deformation modes for the initial and final stages of deformation, being prismatic $\langle a \rangle$ slip the most important deformation mode. Nevertheless, the $\{1100\} \langle 1120 \rangle$ slip does not accommodate deformations in the $\langle c \rangle$ axis direction. The only contribution to $\langle c \rangle$ axis reorientation is due to a local rotation. Then, it is evident that texture evolution is associated to crystal reorientations introduced by twinning.

TABLE I

CASE	ϵ	A C T I V I T Y				
		pr <a>	ttw	ctw	bas <a>	py <c+a>
Cold Rolling	$\epsilon = 5\%$	79 %	17 %	4 %	---	---
	$\epsilon = 10\%$	81 %	11 %	8 %	---	---
	$\epsilon = 25\%$	79 %	10 %	11 %	---	---
	$\epsilon = 50\%$	73 %	12 %	15 %	---	---
	$\epsilon = 100\%$	61 %	17 %	22 %	---	---
Hot rolling	$\epsilon = 5\%$	61 %	---	---	38 %	1 %
	$\epsilon = 50\%$	62 %	---	---	36 %	2 %
	$\epsilon = 100\%$	55 %	---	---	37 %	8 %

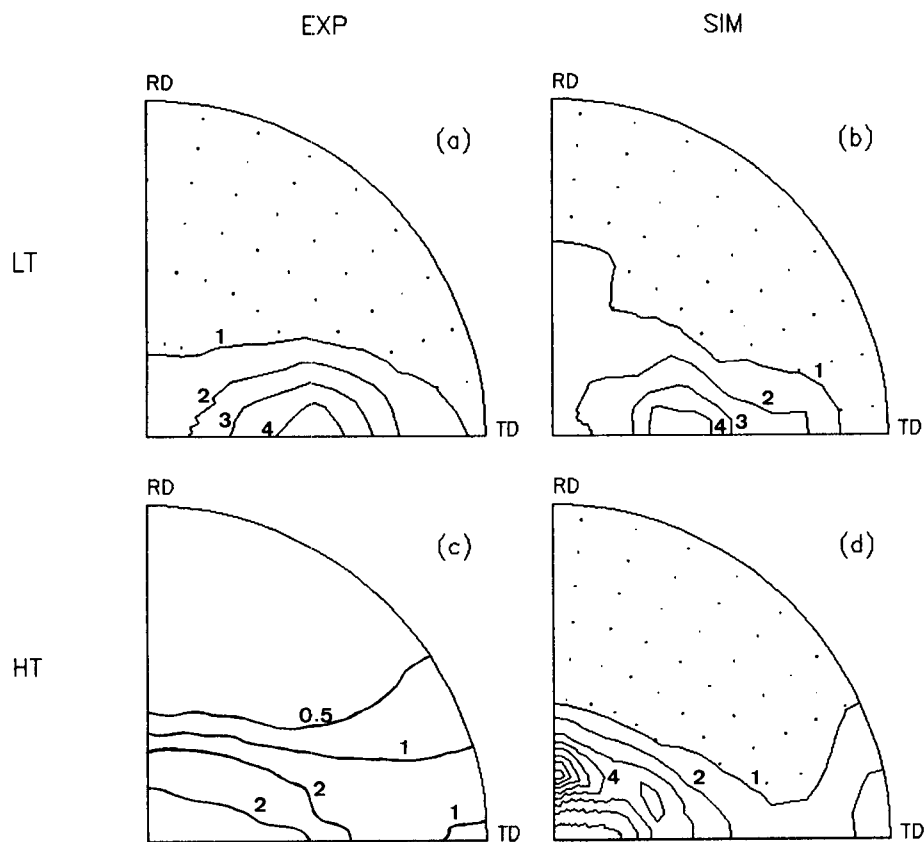


Fig. 1: Experimental and simulated characteristics (0002) Pole Figures for low (LT) and high (HT) temperature rolled Zr alloys.

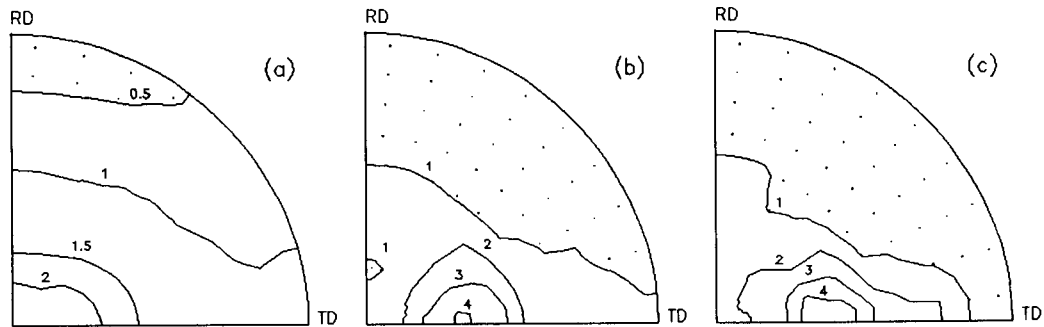


Fig. 2: Prediction of the evolution of (0002) pole figures with rolling deformation: (a) $\epsilon=5\%$; (b) $\epsilon=50\%$; (c) $\epsilon=100\%$.

The predicted evolution of (0002) pole orientations as deformation evolves is presented in Fig. 2. Some aspects of the $\langle c \rangle$ pole axes evolution must be pointed out:

- Pole density presents low values around the RD and reinforcements near the ND for low deformations ($\epsilon \approx 5-10\%$), Fig. 2.a.
- For deformations around $\epsilon \approx 40-50\%$, the typical (0002) pole density reinforcements placed around 30° of the ND in the ND-TD plane begin to be important, Fig. 2.b.
- Afterwards, the only effect of deformation on the texture development is the reinforcement of this component. No significant differences can be observed in (0002) pole figures after $\epsilon=50\%$, Fig. 2.c.

In order to understand the effect of twinning on texture evolution, a detailed study of the reorientations introduced by tensile and compressive twinning was performed. The sequences in Figs. 3.a and 3.c show the $\langle c \rangle$ axes distribution of the volume fraction of grains to be reoriented by twinning at different deformation steps and for different angles ϕ . Level lines represent the volume fraction reoriented by both twinning modes. It is important to remark that the effective twinned volume depends on the texture developed up to the imposed deformation step. On the other hand, sequences in Figs. 3.b and 3.d present a qualitative distribution of the twinned $\langle c \rangle$ axes. Stripped regions exhibit high concentration of twinned $\langle c \rangle$ axes (arbitrary units). The main results indicate that:

- Tensile and compressive twinning are activated in well defined non-overlapped regions of $\langle c \rangle$ axes distribution. Compressive (tensile) twinning is predominant in regions where $\langle c \rangle$ axes are placed near ND (RD) [10].
- The size of the domains associated to the activation of tensile and compressive twinning and the twinned volume fractions for each deformation step change with the accumulated strain introduced by rolling (this is a consequence of the sensitivity of SC model to variations of polycrystal's plastic anisotropy) and with the angle ϕ .
- At the beginning of the deformation process, the activity of tensile twinning is higher than the compressive twinning contribution. This fact allows us to explain the $\langle c \rangle$ axes concentration around ND for low strains.

The formation of the typical reinforcement in the ND-TD plane at $25^\circ-30^\circ$ from the ND can be explained in the following terms:

- 1) The volume fractions of grains to be twinned in tension show a reinforcement for $\phi=25^\circ$ and 35° .

2) Afterwards, secondary tensile twinning takes place inside compressive twins with their $\langle c \rangle$ axes near RD and $\phi \approx 30^\circ$. The final $\langle c \rangle$ axes orientations lie between 20° and 35° from the ND in the ND-TD plane, fig.3.b.

3) These last orientations are stable enough orientations. Comparing with the corresponding Fig. 3.a and 3.c., it can be observed that they cannot be strongly affected by further compressive twinning activity. Then, an accumulation of $\langle c \rangle$ axes is produced for these orientations and, consequently, the associated (0002) pole density increases with rolling deformation.

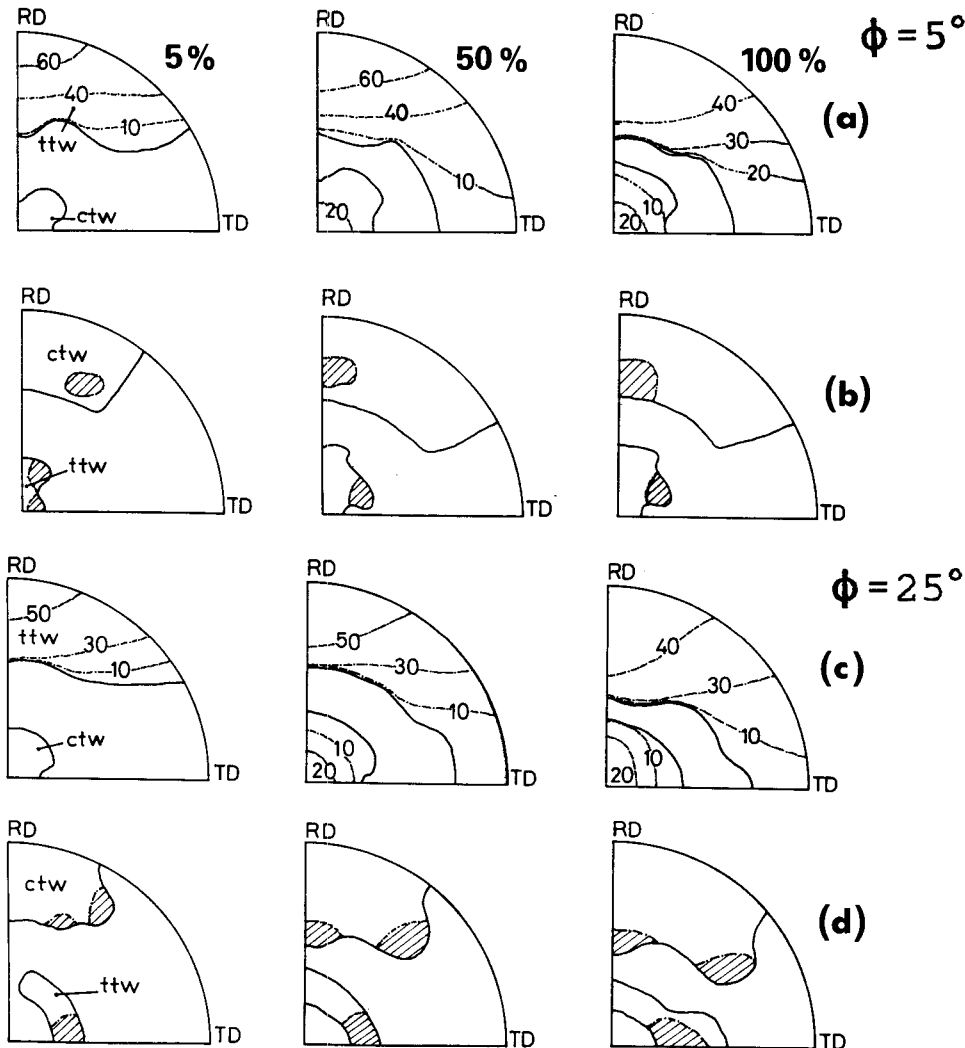


Fig. 3: $\langle c \rangle$ axes reorientations introduced by twinning. Sequences (a) and (c): Distribution of the volume fractions of grains to be reoriented at different deformations steps. Sequences (b) and (d): qualitative distribution of the twinned $\langle c \rangle$ axes (strippes regions correspond to higher concentrations of these axes).

HOT-ROLLING TEXTURES:

Calculations were performed assuming a value $n=7$ of the exponent of the viscoplastic equation [4], meaning that the material becomes more viscous when the temperature rises. This assumption, together with the replacement of twinning systems by slip systems are responsible for the changes in polycrystal plastic behavior. The use of a 'hard' pyramidal $\langle c+a \rangle$ mode leads to simulated textures that are in good agreement with the experimental evidence, Fig.(1). This agreement reveals a coherence between measured values of CRSS, experimental textures and theoretical predictions.

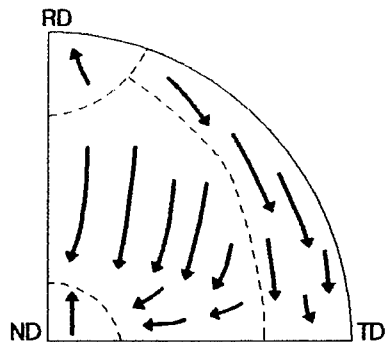


Fig. 4. Mapping of $\langle c \rangle$ evolution during hot rolling

Fig.4 presents a diagram of the evolution of $\langle c \rangle$ axes during texture predictions. Comparing these evolutions, obtained using SC formulation, with experimental and predicted (0002) pole figures, it can be concluded that:

- The $\langle c \rangle$ pole density around RD, which is generated by the activity of $\langle c+a \rangle$ pyramidal slip, disappears with increasing deformations [6].
- The $\langle c \rangle$ axes placed near the RD-TD circle are rotated towards the TD.
- A high basal activity leads to a concentration of the $\langle c \rangle$ axes around ND. The (0002) pole figure presents two maxima near ND, tilted 20° towards RD and TD, respectively.

ACKNOWLEDGEMENTS

This work was partially supported by the Proyecto Multinacional de Investigación y Desarrollo (OEA-CNEA).

REFERENCES

1. Tenckoff, Metall. Trans. A, 1978, 9A, 1401.
2. A. Akhtar, Acta Metallurgica, 1973, 21, 1.
3. A.Pochettino, N.Gannio, C.Vial Edwards, R.Penelle, Scripta Metall.,1992,27,1859.
4. R.Lebensohn, C. Tomé, Acta Metall., in press.
5. C. Tomé, R. Lebensohn, U.F. Kocks, Acta Metall.,1991, 39, 2667.
6. R. Lebensohn, P. Sanchez, A.A. Pochettino, Scripta Metall., to be published.
8. A. Salinas, Ph.D. Thesis, Mc Gill University, 1990.
9. R.G. Ballinger, The Anisotropic Mechanical Behaviour of Zircaloy-2, Garland Publishing Inc., N. York, 1979, 45.
10. E. Tenckoff, Z. Metallk., 1972, 63, 4.